nature energy

ARTICLES

PUBLISHED: 25 JULY 2016 | ARTICLE NUMBER: 16103 | DOI: 10.1038/NENERGY.2016.103

Impacts of climate change on sub-regional electricity demand and distribution in the southern United States

Melissa R. Allen[1]*, Steven J. Fernandez[2], Joshua S. Fu[2,3] and Mohammed M. Olama[1]

High average temperatures lead to high regional electricity demand for cooling buildings, and large populations generally require more aggregate electricity than smaller ones do. Thus, future global climate and population changes will present regional infrastructure challenges regarding changing electricity demand. However, without spatially explicit representation of this demand or the ways in which it might change at the neighbourhood scale, it is difficult to determine which electricity service areas are most vulnerable and will be most affected by these changes. Here we show that detailed projections of changing local electricity demand patterns are viable and important for adaptation planning at the urban level in a changing climate. Employing high-resolution and spatially explicit tools, we find that electricity demand increases caused by temperature rise have the greatest impact over the next 40 years in areas serving small populations, and that large population influx stresses any affected service area, especially during peak demand.

Climate change modelling predicts rising temperatures and consequent increases in storm intensity, flooding and inundation. This poses risks to infrastructure and neighbourhoods as well as disruptions to the energy supply and its dependent infrastructure. Direct effects have already included damage to power plants, roads, bridges and communication towers, and resultant interruption of electrical energy, transportation and communications sectors in cities[1]. As climate conditions continue to change, local communities and their critical infrastructure will respond, adapt and evolve. Population will shift in response to these changes[2,3], for example, as services that generate new economic activity in more environmentally stable locations will attract new workers and associated households. This shift will force demand locations for electricity to change. As a result, networked infrastructures may be required to accommodate new load centres and to minimize vulnerability to natural disasters[4]. To provide information about the complex interactions among climatic conditions, population shifts, and energy supply and use, new tools informed by consistent spatially disaggregated data are needed[5].

Although a recent report began to quantify increases in electricity demand based on regional warming[6], little research has been conducted to quantify the potential impacts of combined climate and population stresses on the operating limits of electrical substations within the power grid. There are two main reasons for this gap. First, until recently, climate projections at high enough resolution to be compatible with infrastructure modelling have been unavailable. Second, spatially explicit population migration data and analysis techniques capable of providing estimates of future energy demand have been missing and/or difficult to characterize.

Previous research has predicted increases in electricity demand in response to increases in global temperature expected with climate change. For instance, using the Electricity Information (EIA) National Energy Modelling System, Hadley *et al.*[7] showed that for most US locations, the savings of electricity in the winter months due to fewer cooling degree days do not offset the added expenditures on electricity in the summer for the increase in heating degree days. The climate inputs used in the Hadley study, however, were global model output at 2.5° (latitude, longitude) spatial resolution, so while the study was able to capture electricity customer response to some general trends in future temperature, it was unable to resolve regional differences in temperature in both base and future cases. To improve on such predictions, the California Energy Commission[8] employed a constructed analogues method for statistically downscaling global climate model output at coarse spatial resolution (2.5°) to finer (~13 km) resolution, using analogues from present regional climate. With this method, along with electricity utility billing data, and demographic information, they made projections regarding increases in residential electricity use.

Although much research regarding population movement has been performed and weaknesses in various methods identified, none of the methods has been applied to the assessment of changes in electricity demand due to spatially explicit changes in population. It has been noted[9] that the growth of every small area is linked to causes and forces located elsewhere in the region and by demographic and economic interactions; thus, the process of regional growth and resulting electricity demand changes is hard to characterize. Yet strides have been made in relating population changes to changes in electricity demand. A variety of commercial models for forecasting electric load based on land use projections have been used to generate scenarios for long-range planning. Among the first were linear urban models based on a gravity model for population movement[10] and generalized

[1]Oak Ridge National Laboratory, Computational Science and Engineering Division, One Bethel Valley Road, PO Box 2008 MS-6017 Oak Ridge, Tennessee 37831-6017, USA. [2]Department of Civil and Environmental Engineering, University of Tennessee, 325 John D. Tickle Building, 851 Neyland Drive, Knoxville, Tennessee 37996-2313, USA. [3]Oak Ridge National Laboratory, Computational Science and Mathematics Division, One Bethel Valley Road, PO Box 2008 MS-6017 Oak Ridge, Tennessee 37831-6017, USA. *e-mail: allenmr@ornl.gov

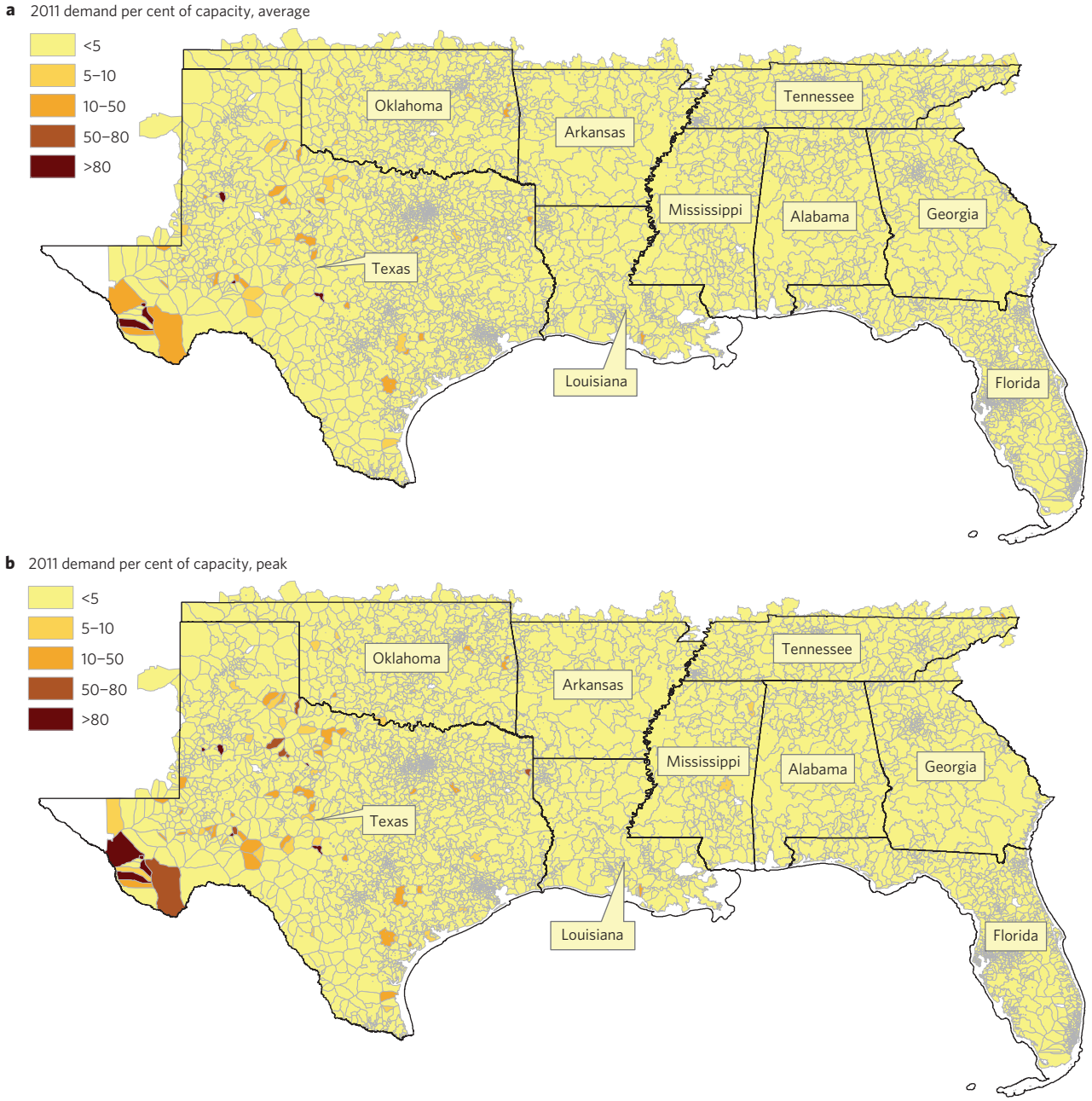

Figure 1 | Per cent substation capacity used by customer service areas in the year 2011. Substation areas are estimated by a cost–distance algorithm that allocates electricity customers to substations on the basis of population density and distance from the station. **a**,**b**, Darker colours indicate a higher percentage of substation capacity for either average (**a**) or peak (**b**) instantaneous demand by customers. The percentage is based on known substation capacity and disaggregated annual state consumption. Peak demand for 2011 is determined on the basis of peak-to-average demand ratios reported by the Electric Reliability Council of Texas (ERCOT) and the Southeastern Reliability Council (SERC). Calculation details are in the Methods.

to a set of matrix computations[11]. While these models take into consideration the projected development of various types of electricity customer (residential, commercial, industrial), they do less well at predicting the ways in which redevelopment of land use will occur. Therefore, the US Geological Survey[12], Duke Energy[13] and the California Energy Commission[14], among others, have expanded such models to incorporate economic and demographic weights for the determination of various redevelopment types using agent-based modelling. For each of these models, the critical components are those of the spatial distribution of the population among their places of residence and their places of business, and the way changes in those distributions are projected for the future. However, these models do not evaluate electricity usage by customers as organized within utility service areas or how service area organization might change as a result of new urbanization.

Vulnerability of the electric grid to climate impacts is ultimately a function of its exposure, its sensitivity and its adaptive capacity to stress[15]. Thus, in this study we examine human response to exposure to changes in regional temperature[16] and increases in landfall hurricane intensity[7,17,18], and electrical grid sensitivity to these human- and climate-induced stresses. We employ a spatial methodology for electric load forecasting for grid planning in which a cost–distance algorithm based on regional population is used to determine the service area for a given substation. We apply satellite population observations and predictions based on Census and Internal Revenue Service (IRS) data to project spatial shifts in

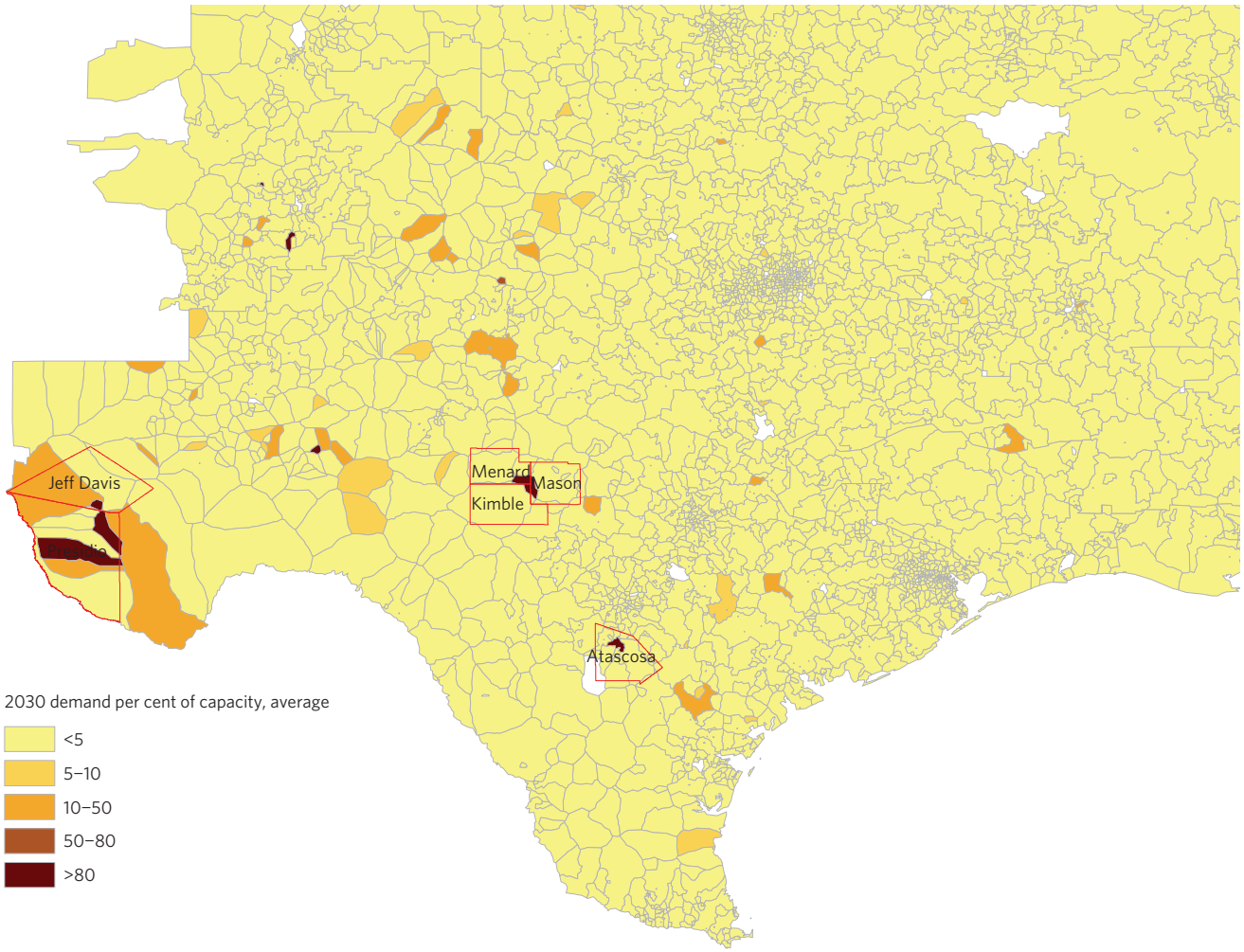

Figure 2 | Per cent of substation capacity of average electricity demand by service area in 2030. Here, we take a closer look at service areas in the state of Texas. Highlighted are those service areas in the sparsely populated counties of Jeff Davis, Presidio, Menard, Mason, Kimble and Atascosa (county boundaries indicated in red) that show greater than 80% of substation capacity needed for average instantaneous demand. This situation is due to increases in population in these sparsely populated regions.

electricity demand in the southern US region (Supplementary Fig. 1) and we incorporate several sudden redistributions of population in response to a 2005-like hurricane season at the predicted return period for such events in the region based on recent climate science. We also calculate local percentage change in electricity demand given temperature changes from dynamically downscaled (12 km resolution) climate model projections for the region to analyse further the effect of increases in global temperature and resulting regional electricity demand consequences. From this analysis, we make a substation-service-area-level projection of substation capability in the southern US to support changes in demand due to temperature rise and sudden population shifts in response to intense storms. This procedure allows us to demonstrate a viable tool for making high-resolution predictions in the absence of address-specific data regarding electricity use.

Demand change with temperature and population change

The focus of our study was to develop a methodology for forecasting high-resolution temperature- and population-related electricity demand increases that may challenge electricity distribution capacity in specific locations Thus, to account for changes in electricity use as a result of changes in population, we use as a first input to the methodology the LandScan[19,20] high-resolution (1 km) satellite-observation-informed population data for average 24-h population locations. We next apply customer correction factors[21] to these totals to aggregate the population to households and firms that represent electricity customers. Finally, we use a cost–distance algorithm to determine electricity customer service areas at the neighbourhood scale for the 2011 population distribution (described in the Methods). To project future customer service areas and demand, we apply these methods to the LandCast[22] population projections (which used cohort-component and appropriate land use predictions and included methods for modelling suitability, service area planning, consequence assessment, mitigation planning and implementation, and assessment of vulnerable populations) to provide reasonable future service areas and planning scenarios. United States Census and other[23] county-level population distribution projections for future years do not factor in environmental stresses caused by climate change (for example, increases in intensity of extreme weather events such as storms), and recent studies have shown not only that significant numbers of people have migrated away from locations affected by extreme storms, but also that these migrations have caused large changes in electricity consumption by counties of both origin (decrease) and destination (increase). Thus, in this study we investigate the impacts of further population redistribution on location-specific electricity demand by including in those projections an adjustment for a 2005-type hurricane season

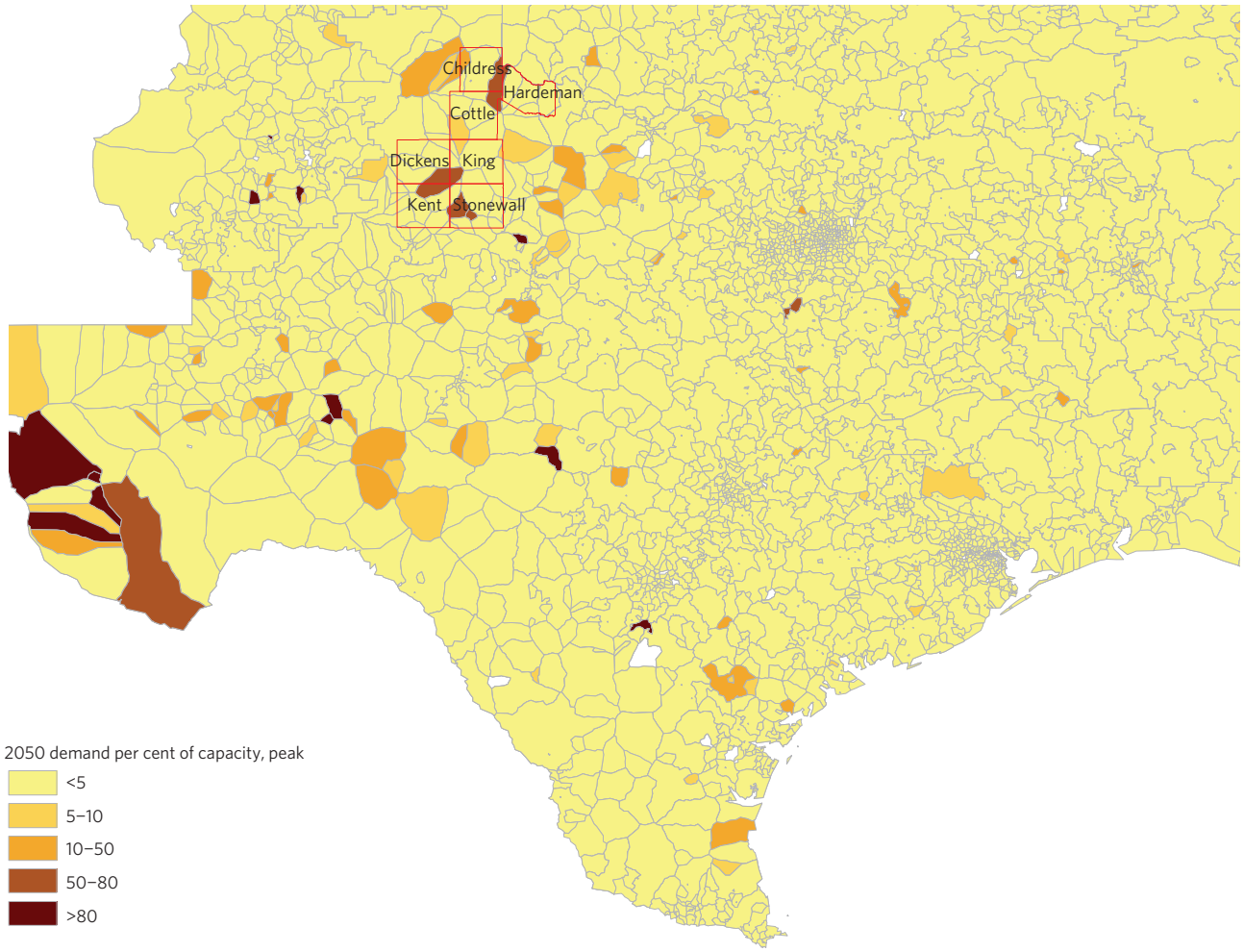

Figure 3 | Per cent of substation capacity of peak electricity demand by service area in the 2050s. Again, we focus on the state of Texas because it is in service areas in this state that we see the most change in demand versus substation capacity due to changes in population as a result of typical projected growth and migration, and to migration away from areas affected by a 2005-like hurricane. In this scenario, counties such as Dickens, King, Kent, Stonewall, Childress, Cottle and Hardeman (county boundaries indicated in red), which operated at much less than 50% capacity for average demand in 2030, operate at between 50% and 80% capacity during peak demand in the 2050s. More service areas in western Texas see demand above 80% capacity for the same reasons.

applied at a hypothetical 20-year return period for such a season[3–5,25]. To simulate this impact, we apply by-county migration rates from 2005–2006 and 2006–2007 to the study region as a hurricane migration component (Supplementary Note 1).

Note that the authors do not attribute hurricanes Katrina, Rita and Wilma to climate change, but use these events as an example scenario to show population changes that could occur under extreme storm circumstances along the US Gulf Coast (a situation that could occur more often in the future due to predicted increases in intensity of storms), and how these circumstances might be represented in a methodology for predicting these changes. (It should also be noted that the largest environmental population redistributions are projected to occur in the least developed countries because those with the most robust economies are more likely to have the means to rebuild[26].)

Recognizing that increased electricity demand in response to rising temperatures has been well established by the utility industry and has a latitudinal dependence[14,27,28], we calculate the percentage increase in electricity demand for a service area due to temperature rise according to a formulation[27] derived from empirical data for the latitudes spanning the state of California. (Although the California data may not provide a direct latitude temperature correlation to the more humid southern US[29], California's constituent climate zones follow a similar latitudinal progression to those in the southern US region[28].) While the constructed analogues statistical downscaling method used in the California Energy Commission study[8] provided enhanced information regarding regional temperature projections, statistical methods tend to be limited by available historical data and past trends. As inputs to these formulae, we instead use results from the Weather Research and Forecasting (WRF) model[30] dynamically downscaled (12 km resolution) from the Community Climate System Model, Version 4 (CCSM4) three-hourly Coupled Model Intercomparison Project, Phase 5 (CMIP5) ensemble member's projections (worst case scenario, Representative Concentration Pathway (RCP) 8.5).

Results from dynamical downscaling methods tend to be more physically, chemically and temporally robust than those of statistical methods because they take into account changes in atmospheric composition and dynamics at small time steps and geographical terrain at small spatial scales, and can follow the non-stationary and evolving climate trends of initial and boundary conditions provided by global model physics. However, there is a range of predictive uncertainty for all variables in the large-scale global models[31], and further uncertainty in dynamically downscaled results[32,33]. We note that CCSM4's output has a slightly-low temperature bias[31], and that WRF output tends toward a high bias for

temperature[32]. That said, this combination of global and regional model has produced historical results in relatively good agreement with the extreme temperature observations for the representative locations in the southern US states considered here (Supplementary Table 1).

New demand map for the southern United States

Projections of future energy capacity and use are made by the EIA for each National Energy Reliability Council (NERC) region for each year from 2011 through 2040[34]. However, these predictions have been unable to identify specific locations of future stresses where local demand may exceed the peak load of substation capacity causing, in extreme climate cases, potential for blackouts. The EIA predicts that each NERC region will sustain a demand between 40–50% of the generating capacity available for each region[34]. Our results improve on these predictions by showing current and future potential vulnerabilities at representative service area locations for individual substations, and demand-to-capacity what-if scenarios for sudden population shifts resulting from storm-driven migration. Additionally, we show the local impact on electricity demand of an overall rise in temperature.

To establish a baseline for these predictions, we first generated a demand map for the southern United States using a cost–distance function (discussed in the Methods) based on the spatial pattern of the location of the population in relation to the electricity substations in service. We then determined the fraction of capacity of the substations that is used on average by customers in a service area assuming per capita usage consistent with the EIA 2011 state average[35]. Figure 1a shows the results of this calculation for average customer demand. Additionally, because it is in the interest of electricity providers to retain enough capacity to serve customers during peak demand hours, we also produced a baseline map that shows the fraction of capacity used for peak demand in 2011 (Fig. 1b, calculation of peak demand described in the Methods). The maps show that if service areas were distributed as the cost–distance function suggests, there would be several service areas in the state of Texas that are operating at 80% or greater substation capacity. The number of these areas increases with the added demand for peak hours.

Next, using the LandCast spatially explicit population projections for the years 2030 and 2050, the same cost–distance function to determine substation service area was applied to allocate the projected populations to the substations. Assuming similar per capita demand to that in 2010, new demand versus capacity was evaluated for years 2030 and 2050 based solely on population growth and redistribution (2030 results are shown in Fig. 2). With this step we show that typical population growth and migration causes little stress to the existing electric grid because such adaptations can be applied in a timely manner even with no additional substation capacity.

A variety of service area locations in Fig. 2 show average demand-to-capacity ratios above 80% including one spanning the sparsely populated Texas counties of Menard, Kimble and Mason; one in Atascosa County, south of San Antonio; and several in the western Texas counties of Jeff Davis and Presidio, both sparsely populated. In peak demand situations, these areas show even larger percentages in demand versus capacity. This result is due in part to the very low substation capacity in these areas. In the case of the substations in northwest Presidio county and in Atascosa county, in which substations hold more than one transmission line connection, the grid becomes even more vulnerable when overall demand spikes[36].

For the decades of both the 2030s and the 2050s, the population distribution effects of a 2005-type hurricane season were simulated on the basis of the rates of in- and out-migration in the IRS data for 2005–2006 and 2006–2007 (procedure described in Supplementary Note 1), and results for peak demand in the 2050s for two years following the hurricane season were calculated using the extrapolated peak-to-average demand ratios described in the Methods (Fig. 3). Here it is assumed that for each county, the approximate ratio of population to the total of residences and firms is maintained from 2011. (In reality, these ratios would change with changes in incoming/outgoing population demographics and incoming/outgoing firm types over time.) When population growth and shifts due to hurricane displacement are taken into account, service areas in the Texas counties of Dickens, King, Kent, Stonewall, Childress, Cottle and Hardeman operate at between 50 and 80% capacity during peak demand.

Table 1 | Percentage increase in demand from 2011 to 2030 and 2050 due to increase in July maximum temperature.

	2030			2050		
State	Minimum	Maximum	Mean	Minimum	Maximum	Mean
Texas	4.1	12.1	8.3	8.7	43.1	25.3
Louisiana	6.5	13.7	9.5	10.5	35.8	20.7
Oklahoma	2.9	8.2	5.3	21.3	44.7	33.1
Arkansas	2.9	8.2	6.2	21.3	44.7	33.1
Mississippi	5.1	12.0	7.5	17.2	34.2	24.0
Alabama	4.5	10.2	6.5	11.5	35.4	22.5
Georgia	3.4	9.8	5.7	5.9	24.2	18.1
Tennessee	4.8	8.2	6.5	6.0	31.4	18.1
Florida	6.5	11.6	8.6	−2.5	31.8	12.5

*Minimum, maximum and mean values among the service areas in each state are shown.

Finally, calculations for increase in electricity demand due to increases in highest July temperature predictions were made (detailed in the Methods). The differences in highest July temperature from 2004–2057 in each of the (sub-county) service areas (found by assigning to each service area the average of the temperature in the grid cells that fall within a service area) are normally distributed and range from −0.4 to 9.2 °C. These differences in summer high temperatures have a large impact on electricity demand[37], as can be seen in Table 1, and strain available capacity at peak demand. This is seen most prominently in the service areas identified in Fig. 3 as having substations operating at 50–80% capacity during peak load. As the temperature rises, the average demand on these substations increases to over 80% of capacity.

Figure 4 shows the demand difference due to temperature change, population growth and population movement for the 2050s with two hurricane displacements applied. This figure was created by taking the difference in each spatial location of the percentage demand of substation capacity calculated for 2050s and that calculated for the 2011 base case. Service areas with large decreases in demand located next to service areas with large increases in demand are shown for several service areas in locations of low population in Texas. Within the more densely populated areas of Texas—Dallas, San Antonio and Houston—there is little change in percentage demand of capacity. Sparsely populated locations in Oklahoma, Mississippi, Alabama, Tennessee, Georgia and Florida show up to 10% increases in projected demand. Only one small service area in the centre of Arkansas shows an increase in demand. All of these results are likely to be due primarily to the combination of low-capacity substations and the pattern of population growth projected for those regions, although some of the increase is explained by increases in maximum temperature.

Discussion

The use of high-resolution population distribution data and dynamically downscaled climate projections with electricity demand modelling provides an improved method for identifying

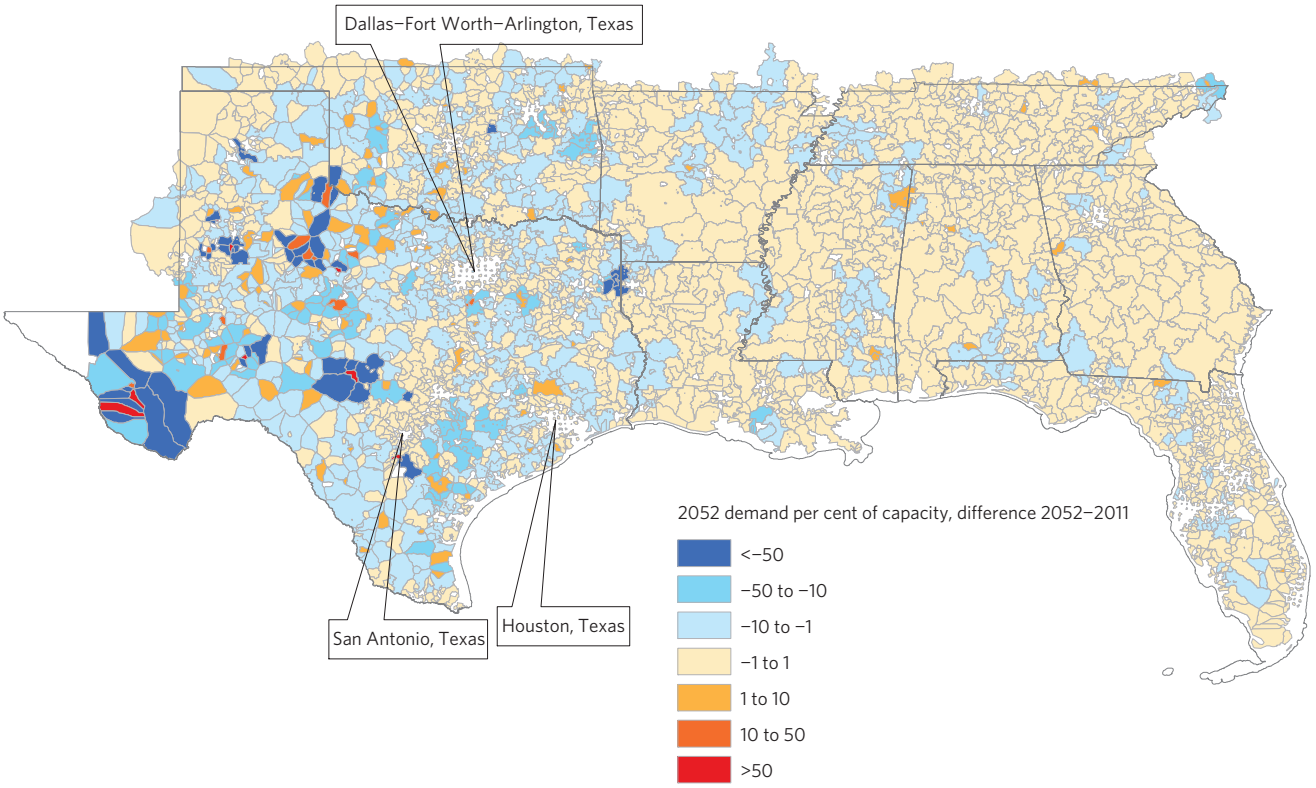

Figure 4 | Difference in demand percentage of capacity, 2052–2011. With changes in temperature due to climate change in addition to migration, large changes in electricity demand as compared with substation capacity are evident throughout the southern US. The largest changes are seen in service areas serving smaller populations in Texas, with adjacent service areas seeing differences larger than ±50%.

specific locations of electrical grid vulnerability to increased electricity demand due to regional temperature changes, and to large population shifts. Using a representative data set of 12 km dynamically downscaled RCP 8.5 (worst case) temperature projections and business-as-usual population projections, with an added hurricane migration component, our results show that electricity demand increases due to temperature change are slightly less than those due to large population influx into a service area, but that in the areas most affected, and especially at peak demand, the grid will be stressed. It is also evident that some sections of the national electrical grid are more adaptable to population shifts and changing demand than other sections are; and that detailed projections of changing local electricity demand patterns are important for planning at the urban level. Until this time, however, it was an open question whether these population shifts could be modelled with realistic coupling to climate forecasts.

The findings from this study show that new population data enabled by high-resolution imagery analysis not previously available at this scale (1 km) can be operationalized for planning professionals. A long-standing challenge has been helping those who project new grid networks of critical infrastructures to understand implications of climate events by accessing, displaying and using newly available data and coupled models. The models of geographic distribution of projected electric power demand grow increasingly unrealistic if based only on current assets. These planners at regional utilities often are charged with reorganizing substation service areas, capacity upgrades to existing substations, and adding and removing substations as the grid evolves in response to changing demand. This study also illustrates that analysts and modellers should add population movements as a component to be modelled when projecting future infrastructure climactic stresses. For some neighbourhoods, the population shifts motivated by economic opportunity dominate ambient environmental stresses to engineered infrastructure. The data support the feasibility of exploring different scenarios and assumptions within a population–climate coupled system. Additionally, as more highly resolved data become available, further analysis using this methodology can yield more detailed results for future planning.

Projecting other factors and system changes continues to be a challenge. Some factors continue to create difficulties such as projecting technological change and institutional change. Thus, the research community should continue to plan efforts to depict a range of changes in socioeconomic conditions through time (for example, using shared socioeconomic pathways[38]) and their impacts on demand for resources, just as climate scenarios (RCPs) based on anthropogenic forcing depict a range of changes in future climate conditions.

Methods

Electricity supply and demand data sources. Data sets used for the determination of changes in electricity demand due to changes in population include substation location and measured capacity (data from Ventyx corporation included in the layers developed for the Homeland Security Infrastructure Program (HSIP) in 2013) LandScan population data sets for 2011[19,20] and projections for 2030 and 2050[22]; EIA State Energy Data System[35] state-by-state total annual electricity consumption records for 2011 and the Annual Energy Outlook (2013) predictions to 2040; and IRS[39] data sets for by-county in- and out-migration for the years 2004–2007.

Spatially explicit population data and projections. The 2011 LandScan[2,19] data set is built using a dasymetric mapping approach in which a source layer is converted to a surface and multiple ancillary indicator data layers are used to derive density level values for input to a weighting scheme that allocates population to 1 km grid cells. The source data layer surface comprises the subnational level census counts. Ancillary data sets include primary geospatial data such as land cover, roads, slope, urban areas, village locations and high-resolution imagery analysis; all of which are key indicators of population distribution. Calculation of error in the data set is made by imagery analysts

using high-resolution imagery to create a set of population likelihood coefficient modifications to correct or limit input data anomalies. Population projections for 2030 and 2050 are made in a similar manner, but also incorporate cohort-component and urbanization projections as outlined by the US Census[22]. However, as uncertainty is intrinsic in all population predictions, and especially those for small geographic units, we note the uncertainty in these projections as well. Results from a comparison of predictions made using the LandCast methodology from the 2000 Census report to the 2010 Census report showed that county-level predictions were overestimated by as much as 3.72%. This discrepancy is partially explained by the fact that the LandCast predictions were only 'business as usual' and did not take into account migration due to natural disaster (for example, 2005 hurricane season) or economic downturn (for example, Detroit from 2005) during that decade. An example of anticipated changes in population density for mid century is shown in Supplementary Fig. 2. Projections indicate overall population growth along with movement away from rural areas and larger concentrations in cities and suburbs.

Average customer demand per service area. To determine the amount of stress placed on substation capacity in an area and to estimate the service area for each substation based on its location and its capacity, we used a two step process: convert LandScan population count to customer count[21]; and employ a cost–distance algorithm[40] to allocate customers to the substations most likely to serve them.

For each county, a customer correction factor was obtained by adding together the number of households and the number of firms within the county as given by the US Census for the year 2000, and then dividing the total population in the county for that year by this sum[21]. To convert the population in a given 1 km cell to customers, then, the population was divided by the customer correction factor. While this calculation does not represent a perfect relationship between population and customers, in that it does not account for the differences in electricity use characteristics among residential, industrial and commercial customers (nor the change in number of residences and firms through time), it does offer a simple means for disaggregating average use across all sectors with a representative case.

The cost–distance algorithm[40] employed compares cost units to geographical units to determine the maximum distance to customers served. In this approach, the lower the demand, the higher the cost, and the greater the transmission distance, the greater the cost.

To project the total average customer instantaneous demand per service area for the future, we take as a base average per-customer demand value the total consumption in gigawatt hours per year per state divided by the number of customers in the state and then further divided by the number of seconds in a year (365.25 × 24 × 3,600) and multiply by 1,000 to convert gigawatts to megawatts. Once the average customer instantaneous demand is calculated, we calculate the total customer demand per substation service area by multiplying this value by the number of customers within the service area. Substation capacity for a service area is estimated using measurements of the instantaneous aggregate peak load (real and reactive power) at the substation for a typical summer day to obtain the instantaneous aggregate apparent power at each substation and assuming that it is approximately 80% of the total capacity.

Determining service areas for the substations. The service areas are determined using a cost–distance algorithm within a Geographic Information Systems (GIS) framework. The service area cost is computed with the following equation, where P is the population of a given 1 km cell in the LandScan data set, $\sum$ is the sum of the population in a study region and S is the capacity sum of the substations in the region. Study regions are bounded by North American Electricity Reliability Corporation (NERC) sub-region borders. The historical electricity consumption data on which we calibrated the base case were given at county and state levels, however, so GIS spatial joining was used to map demand to each derived service area.

$$D_{\mathrm{inv}} = \frac{1}{\frac{P}{\sum P} \times S} \tag{1}$$

Geographical cells are allocated to a given substation on the basis of the lowest accumulated cost to reach the source from the cell. Accumulated cost is calculated as the sum of two values: c1 is the average of D_{inv} for the starting cell and the ending cell; and c2 is the average of D_{inv} for the starting cell and the midpoint cell (Supplementary Fig. 3).

For diagonal transmission distance travelled, distance between cells increases to the length of the diagonal, in this case, $\sqrt{2} = 1.414$, so each average value is multiplied by this amount. Cells that contain the substations, or source cells, are given a D_{inv} value of 0. Since no D_{inv} calculation can be made from the 'no data' cells, these cells act as barriers to the movement of the allocation process. Cost allocation is performed as an iterative process beginning with the cost evaluation of the source cell, and then extending to the eight neighbouring cells of the source cell (Supplementary Fig. 4). For each concentric square of cells, the cells that help form the least cost path outward from the source are added to the service area of the source. Changing of allocated cells is possible, for instance, if a new, cheaper route is found by adjusting choices on inner squares to access less expensive cells on outer squares. This process continues until all of the cells are allocated, or an optional maximum distance threshold is met.

Substation capacity measurements and estimates. Substation capacities (Supplementary Fig. 5) are estimated using measurements of the instantaneous aggregate peak loads at substations for a typical summer day in the year of 2011 (proprietary data courtesy of the Tennessee Valley Authority (TVA) and Electricity Reliability Council of Texas (ERCOT)). The measurements are load real powers, P, in megawatt and load reactive powers, Q, in mega VAR (volt ampere reactive). Then, the apparent power, AP, in mega volt ampere (MVA) for each substation is computed as

$$\mathrm{AP} = \sqrt{(P^2 + Q^2)} \tag{2}$$

and we assume that the substation peak apparent power in a typical summer day is approximately 80% of the total substation capacity. In this case, the apparent power values are multiplied by 1.25 to obtain an approximation for the total substation capacities.

Peak customer demand per service area. For an electric utility company, peak demand is defined as the single half-hour or hour-long period during which the highest amount of customer consumption of electricity occurs. Since the amount of electricity over a certain threshold must often be purchased from additional providers during this time, the cost to provide that electricity can be much more than that produced up to that threshold. Therefore, the utility companies calculate a peak-to-average demand ratio to be used in assessing their own costs to provide the electricity and the costs they pass on to the consumers. This amount is found by relating the peak of the electricity use curve to the area underneath the curve. Assuming Gaussian distribution and area A, the height of the peak is:

$$H = f(\mu) = \frac{A}{\sigma\sqrt{2\pi}} \mathrm{e}^{-(\mu-\mu)^2/2\sigma^2} = \frac{0.3989A}{\sigma} \tag{3}$$

$$\frac{H}{A} = \frac{0.3989}{\sigma}, \quad \sigma = \frac{\mathrm{FWHM}}{2.35} \tag{4}$$

and FWHM (full-width at half-maximum) measured in the data from the utility readings.

The peak-to-average demand ratios calculated by ERCOT and by SERC for the years 1993–2012 are shown in Supplementary Figs 6 and 7. To these time series, we fit a linear trend to project peak-to-average demand ratios for future years, 2030 and 2050. With this information, we calculate peak demand for those years for each of the states (ERCOT values for Texas, SERC values for the other states) included in our southern study region. It should be understood that the years 2030 and 2050 are only representative years for those decades, and thus a more exact fit to the more cyclical nature of the peak-to-average demand ratios is not necessarily required for the approximation.

Demand change in response to temperature rise. Increased electricity demand in response to rising temperatures has been well established by the utility industry, and it has a latitudinal dependence. The per cent increase in electricity demand for a county due to temperature rise is calculated according to[27]

$$J = (5.33 - 0.067L_{\mathrm{centroid}}) \times \Delta T \tag{5}$$

where J is per cent increase in electricity demand, L_{centroid} is the latitude in decimal degrees at the centroid of the county and ΔT is the change in maximum annual temperature in degrees Fahrenheit.

New demand as a result of this increase is calculated:

$$D = D_{\mathrm{av}} \times N \times \left(1 + \frac{J}{100}\right) \tag{6}$$

where D is the total demand for the study area, D_{av} is the average customer use and N is the number of customers.

As temperature input to these formulae, we enter dynamically downscaled historical and Representative Concentration Pathway scenarios (RCP 8.5) using initial and boundary conditions generated by the Coupled Model Intercomparison Project, Version 5 (CMIP5) ensemble member, Community Earth System Model (CESM), at three-hour intervals for Weather Research and Forecasting (WRF) domain simulations at 12 km resolution centred at 97° W,

40° N (ref. 30). The WRF 12 km data sets are then incorporated as dBASE file tables into a GIS platform, projected to a common coordinate system (WGS84 as in LandScan) and joined to additional energy and infrastructure layers (also projected to WGS84). A simple analysis of variance comparison of daily maximum temperatures from the National Climatic Data Center (NCDC) observations and the 2001–2004 WRF-downscaled base case data set is shown in Supplementary Table 1. Observation stations are Atlanta Hartsfield International Airport, Louisiana State University Ben Hur Farm, Houston William P Hobby Airport, Huntsville International Airport, Jackson International Airport, North Little Rock Airport the Memphis Weather Forecast Office, Miami International Airport and Tulsa International Airport, respectively. Daily maximum temperature observations for Houston, Huntsville, Jackson and Little Rock match the model output less well than those at the other stations, possibly because urban/airport effects are not yet well captured in the WRF model. Supplementary Figs 7–15 show raw data comparisons of modelled and measured data for each location. While it is evident that the model captures the range of the temperatures at each location and the seasonal trend, predictions for a specific day of the year are not expected to be exact.

Hurricane intensity and frequency under climate change. Studies[17,18] indicate that increases in intensity of hurricanes will characterize the climate of the latter half of the twenty-first century. Their calculation of power dissipation index for 2006–2100 shows an increase of 0.5×10^8 m^3 s^{-2} in the Gulf Coast region. This prediction upgrades tropical depressions, tropical storms and hurricanes as outlined in Supplementary Table 2. In general, damage rises by about a factor of four for every category increase[41]; thus, population stresses associated with hurricanes are likely to increase with the increase in hurricane intensity.

Received 30 December 2015; accepted 16 June 2016; published 25 July 2016

References

1. Wilbanks, T. J. & Fernandez, S. J. *Climate Change and Infrastructure, Urban Systems, and Vulnerabilities* Technical Report for the US Department of Energy in Support of the National Climate Assessment (Oak Ridge National Laboratory, 2012); http://www.esd.ornl.gov/eess/esd_fact_sheets/Infrastructure022912.pdf
2. McGrananhan, G., Balk, D. & Anderson, B. The rising tide: assessing the risks of climate change and human settlements in low elevation coastal zones. *Environ. Urban* **19**, 17–37 (2007).
3. Warner, K., Erhart, C., de Sherbinin, A., Adamo, S. B. & Chai-Onn, T. *In Search of Shelter: Mapping the Effects of Climate Change on Human Migration and Displacement* (United Nations University, CARE and CIESIN-Columbia Univ., 2009).
4. Benson, C. & Clay, E. *Understanding the Economic and Financial Impact of Natural Disasters. The International Bank for Reconstruction and Development* (The World Bank, 2004).
5. Dilley, M., Chen, R. S., Deichmann, U., Lerner-Lam, A. L. & Arnold, M. *Natural Disaster Hotspots: A Global Risk Analysis* (The World Bank, 2005).
6. Kopp, R. *et al. The American Climate Prospectus: Economics Risks in the United States* (Rhodium Group, 2014); http://climateprospectus.org/publications
7. Hadley, S. W., Erickson, D. J. III & Hernandez, J. L. Responses of energy use to climate change: a climate modeling study. *Geophys. Res. Lett.* **33**, L17703 (2006).
8. Hidalgo, H. G., Dettinger, M. D. & Cayan, D. R. *Downscaling with Constructed Analogues: Daily Precipitation and Temperature Fields Over the United States* PIER Final Project Report CEC-500-2007-123 (California Energy Commission, 2008).
9. Batty, M. The size, scale, and shape of cities. *Science* **319**, 769–771 (2008).
10. Lowry, I. S. *A Model of Metropolis* Memorandum RM-4035-RC (The RAND Corporation, 1964); https://www.rand.org/content/dam/rand/pubs/research_memoranda/2006/RM4035.pdf
11. Garin, R. A. A matrix formulation of the Lowry model for intrametropolitan activity location. *J. Am. Inst. Plan.* **32**, 361–364 (1966).
12. Clarke, K. C. & Leonard, J. G. Loose-coupling a cellular automation model and GIS: long-term urban growth prediction for San Francisco and Washington/Baltimore. *Lect. Notes Comput. Sci.* **12**, 699–714 (1998).
13. *LoadSEERTM Spatial Electric Expansion & Risk* (Integral Analytics, 2010); http://www.integralanalytics.com/files/documents/related-documents/LoadSEER.pdf
14. Auffhammer, M. & Aroonruengsawat, A. *Hotspots of Climate-Driven Increases in Residential Electricity Demand: A simulation Exercise Based on Household Level Billing Data for California* White Paper CEC-500-2012-021 (California Energy Commission, 2012); http://www.energy.ca.gov/2012publications/CEC-500-2012-021/CEC-500-2012-021.pdf
15. IPCC *Climate Change 2007: Impacts, Adaptation and Vulnerability* (eds Parry, M. L., Canziani, O. F., Palutikof, J. P., van der Linden, P. J. & Hanson, C. E.) 23–78 (Cambridge Univ. Press, 2007).
16. IPCC *Climate Change 2013: The Physical Science Basis* (eds Stocker, T. F. *et al.*) (Cambridge Univ. Press, 2013).
17. Emanuel, K. Increasing destructiveness of tropical cyclones over the past 30 years. *Nature* **436**, 686–688 (2005).
18. Emanuel, K. A. Downscaling CMIP5 climate models shows increased tropical cyclone activity over the 21st century. *Proc. Natl Acad. Sci. USA* **110**, 12219–12224 (2013).
19. Bhaduri, B. L., Bright, E., Coleman, P. & Urban, M. LandScan USA: a high resolution geospatial and temporal modeling approach for population distribution and dynamics. *GeoJournal* **69**, 103–117 (2007).
20. Cheriyadat, A., Bright, E. A., Bhaduri, B. L. & Potere, D. Mapping of settlements in high resolution satellite imagery using high performance computing. *GeoJournal* **69**, 119–129 (2007).
21. Young, B. S., Fernandez, S. J. & Omitaomu, O. A. *Dynamic Modeling of Components on the Electric Grid* Report ORNL/TM-0000/00 (Oak Ridge National Laboratory, 2009).
22. McKee, J. J., Rose, A. N., Bright, E., Huynh, T. & Bhaduri, B. L. A locally-adaptive, spatially-explicit projection of US population for 2030 and 2050. *Proc. Natl Acad. Sci. USA* **112**, 1344–1349 (2015).
23. Mays, G. T. *et al. Application of Spatial Data Modeling and Geographical Information Systems (GIS) for Identification of Potential Siting Options for Various Electrical Generation Sources* Technical Report ORNL/TM-2011/157/R1 (ORNL, 2012).
24. Allen, M. R., Fernandez, S. J., Fu, J. S. & Walker, K. A. Electricity demand evolution driven by storm motivated population movement. *J. Geogr. Nat. Disast.* **4**, 126 (2014).
25. Keim, B. D., Muller, R. A. & Stone, G. W. Spatiotemporal patterns and return periods of tropical storm and hurricane strikes from Texas to Maine. *J. Clim.* **20**, 3498–3509 (2007).
26. Noy, I. The macroeconomic consequences of disasters. *J. Dev. Econ.* **88**, 221–231 (2009).
27. Toole, G. L. *et al.* Effects of climate change on California energy security. *Int. Symp. Systems and Human Science* LA-UR-06-0984 (America Analytics, 2006); http://almeriaanalytics.com/articles-and-white-paper-2
28. United States Department of Agriculture (USDA) *Plant Hardiness Zone Map* (Agricultural Research Service, accessed 3 June 2016); http://www.almanac.com/content/plant-hardiness-zones
29. Deschenes, O. & Greenstone, M. Climate change, mortality, and adaptation: evidence from annual fluctuations in weather in the US. *Am. Econ. J. Appl. Econ.* **3**, 152–185 (2011).
30. Gao, Y., Fu, J. S., Drake, J. B., Liu, Y. & Lamarque, J.-F. Projected changes of extreme weather events in the eastern United States based on a high resolution climate modeling system. *Environ. Res. Lett.* **7**, 044025 (2012).
31. Flato, G. *et al.* in *Climate Change 2013: The Physical Science Basis* (eds Stocker, T. F. *et al.*) 741–866 (IPCC, Cambridge Univ. Press, 2013).
32. Vrac, M. *et al.* Dynamical and statistical downscaling of the French Mediterranean climate: uncertainty assessment. *Nat. Hazards Earth Syst. Sci.* **12**, 2769–2784 (2012).
33. Trzaska, Y. & Schnarr, E. *A Review of Downscaling Methods for Climate Change Projections* (USAID, 2014).
34. *Annual Energy Outlook (AEO): 2005–2040* (EIA, accessed 18 August 2015); http://www.eia.gov/forecasts/aeo/data.cfm
35. *State Energy Data System (SEDS): 1960–2012 (Complete)* (EIA, accessed 18 August 2015); http://www.eia.gov/state/seds/seds-data-complete.cfm
36. Demsar, U., Spatenkova, O. & Virrantaus, K. Identifying critical locations in a spatial network with graph theory. *Transact. GIS* **12**, 61–82 (2008).
37. Edenhofer, O. *et al.* (eds) *Special Report on Renewable Energy Sources and Climate Change Mitigation. Prepared by Working Group III of the Intergovernmental Panel on Climate Change* (Cambridge Univ. Press, 2011).
38. O'Neill, B. C. *et al.* A new scenario framework for climate change research: the concept of shared socioeconomic pathways. *Clim. Change* **122**, 387–400 (2014).
39. *SOI Tax Stats County-to-County Migration Data Files* (Internal Revenue Service, accessed 18 August 2015); http://www.irs.gov/uac/SOI-Tax-Stats-County-to-County-Migration-Data-Files
40. Omitaomu, O. A., Fernandez, S. J. & Bhaduri, B. L. *Handbook of Emergency Response: A Human Factors and Systems Engineering Approach* (eds Adedeji, B. B. & LeeAnn, R.) (CRC Press, 2013).
41. Pielke, R. A. Jr *et al.* Normalized hurricane damage in the United States. *Nat. Hazards Rev.* **9**, 29–42 (2008).

Acknowledgements

This manuscript has been authored by employees of UT-Battelle, under contract DE-AC05-00OR22725 with the US Department of Energy. The authors would also like to acknowledge the financial support for this research by the Integrated Assessment Research Program of the US Department of Energy's Office of Science. We thank the Tennessee Valley Authority and Electric Reliability Council of Texas for their provision of power data to the project.

Author contributions

M.R.A., S.J.F. and J.S.F. designed the study. M.R.A. collected the population, migration and electricity consumption data and performed the service area and per cent demand calculations. J.S.F. provided the climate and WRF-downscaled temperature data and analysis. M.M.O. acquired, archived, documented and analysed the substation capacity data. All participated in drafting, reviewing and revising the manuscript.

Additional information

Supplementary information is available online. Reprints and permissions information is available online at www.nature.com/reprints. Correspondence and requests for materials should be addressed to M.R.A.

Competing interests

The authors declare no competing financial interests.